CORA Cork Open Research Archive
Cartlann Taighde Oscailte Chorcaí

Title	Towards thiol functionalization of vanadium pentoxide nanotubes using gold nanoparticles
Authors	Lavayen, Vladimir;O'Dwyer, Colm;Cardenas, G.;Gonzalez, Guillermo;Sotomayor Torres, Clivia M.
Publication date	2006-09-15
Original Citation	Lavayen, V., O' Dwyer, C., Cardanes, G., Gonzalez, G. and Sotomayor Torres, C. M. (2007) 'Towards thiol functionalization of vanadium pentoxide nanotubes using gold nanoparticles'. Material Research Bulletin, 42(4), pp. 674–685. http://www.sciencedirect.com/science/article/pii/S0025540806003175
Type of publication	Article (peer-reviewed)
Link to publisher's version	http://www.sciencedirect.com/science/article/pii/S0025540807005272 - 10.1016/j.materresbull.2006.07.022
Rights	© 2006 Elsevier Ltd. All rights reserved. This manuscript version is made available under the CC-BY-NC-ND 4.0 license - http://creativecommons.org/licenses/by-nc-nd/4.0/
Download date	2024-04-25 13:44:05
Item downloaded from	https://hdl.handle.net/10468/2848

UCC
University College Cork, Ireland
Coláiste na hOllscoile Corcaigh

Towards Thiol Functionalization of Vanadium Pentoxide Nanotubes using Gold Nanoparticles

V. Lavayen,[†] C. O'Dwyer,[†] G. Cárdenas,[a] G. González,[‡] and C. M. Sotomayor Torres[†]

[†] *Tyndall National Institute, University College Cork, Lee Maltings, Cork, Ireland*

[‡] *Department of Chemistry, Faculty of Science,*

Universidad de Chile, P.O. Box 653, Santiago, Chile and

[a] *Departamento de Polimeros, Facultad de Ciencias Quimicas,*

Universidad de Concepción, P.O. Box 160-C, Concepción, Chile

Abstract

Template-directed synthesis is a promising route to realize vanadate−based 1-D nanostructures, an example of which is the formation of vanadium pentoxide nanotubes and associated nanostructures. In this work we report the interchange of long-chained alkyl amines with alkyl thiols. This reaction was followed using gold nanoparticles prepared by the Chemical Liquid Deposition (CLD) method with an average diameter of ∼0.9 nm and a stability of ∼85 days. V_2O_5 nanotubes (VOx-NTs) with lengths of ∼2 μm and internal hollow diameters of 20−100 nm were synthesized and functionalized in a Au-acetone colloid with a nominal concentration of ∼4 $\times$ 10^{-3} mol dm^{-3}. The interchange reaction with dodecylamine is found only to occur in polar solvents and incorporation of the gold nanoparticles is not observed in the presence of *n*-decane.

KEYWORDS: A. nanostructures, B. chemical synthesis, C. electron diffraction, C. electron microscopy, D. optical properties

I. INTRODUCTION

The template-directed synthesis is a promising route to realize 1-D nanostructures, because it offers the possibility to design and create nanotubes, nanowires and other associated nanostructures, with specific electronic and optical properties [1]. This is demonstrated by the increasing body of work describing the formation and morphology of nanotubes prepared using this approach [2–8]. An pertinent example is the work of Nesper *et al.* [2, 3] who reported the formation of vanadium pentoxide nanotubes (VOx-NTs) using long alkyl primary amines and other varieties of amines [1] as direct structural agents. One of the current applications of vanadate-based nanocomposites is their incorporation in secondary Li-batteries [1, 3] following several reports of metal cation insertion in vanadate-based compounds [1, 5, 7, 8].

A new direction for the application of nanostructure research is their employment as optical materials. Indeed, vanadium oxide nanotubes are already becoming an important optoelectronic material [1] for non-linear optics and have been found to exhibit unique anisotropic properties [3, 6]. These can exhibit intensity dependent transmission and are of central interest in the field of nonlinear optics and optoelectronics because of their potential application in a wide variety of optical systems. In particular, optically active nanoparticles have gained tremendous importance in this field because they exhibit very little Rayleigh scattering in the visible spectrum and thus exhibit optical limiting characteristics [9]. The drive to incorporate metal nanoparticles in nanostructured systems [9] in order to observe the relation between the suitability/compatibility of these systems and biological molecules [10], has opened a new direction for functionalized nanotube research with promising potential applications. The incorporation of nanoparticles in carbon nanotubes has been reported [10]

and the attachment of biological molecules to these nanotubes by different methods has also been realized [10, 11].

Nanoparticle incorporation in vanadium oxide nanocomposites, in particular VOx-NTs, has not yet been realized and this work reports the first successful functionalization of V_2O_5 nanostructures with Au nanoparticles. While metallic colloids are well known, non-aqueous systems enjoy more recent attention because their properties are different to the bulk material and at the same time different to the atomic state with intermediate electronic properties [12]. Another important property is that nanometric particles possess a large fraction of atoms localized on the surface, producing unique and unusual properties; indeed we previously reported [13] the preparation and formation of stable metallic colloids in organic solvents at low temperature. The colloidal particles thus obtained are not only stable at room temperature but in addition, they are also free of impurities [14].

In this paper, we report the first observation of successful thiol functionalization of vanadium pentoxide nanotubes using a new method of functionalization by means of Au nanoparticles with an average diameter of 0.9 nm. Using the Chemical Liquid Deposition method, the reaction was amenable to *in-situ* observation and such a new technique is critical for the successful functionalization of the next generation of nanotubular materials with unique optical and electrical properties.

II. EXPERIMENTAL

A. Synthesis of Vanadium Pentoxide Nanotubes (VOx-NTs)

The method employed for the synthesis of vanadium pentoxide was essentially the one described in Refs [1–6] with some variations. A mixture of *t*-butyl alcohol and orthorhombic

V_2O_5 was refluxed for 6 h to form the xerogel [6, 15]. Water was added to the resulting dark yellow solid and the remaining *t*-butyl alcohol was removed with excess water in vacuum. Water was then added to yield a suspension. The material was aged at room temperature yielding a red-brown colloidal V_2O_5. The xerogel and a primary amine, dodecylamine (DDA), mixed in a molar ratio of 1:2 were stirred in ethanol for 2 h and left to age for 2 days. The composite was transferred into a Teflon-lined autoclave and held at 180°C for 3 days under auto-generated pressure in a sand bath. The product was washed with deionized water and alcohol several times and dried under vacuum.

B. Preparation of the Au-acetone Colloid

The metal atom reactor (3L) used was described elsewhere [12–14]. As a typical example of preparation, 70 mg of Au metal was placed into the alumina-tungsten crucible. Dry acetone was placed in a ligand inlet tube and freeze-pump-thaw degassed in several cycles. The reactor was pumped down to 4−5 mm Hg, while the crucible was warmed to red heat. The surrounding vessel was cooled with liquid nitrogen and Au and acetone (100 ml) were deposited for a period of 1 h. The matrix was allowed to warm under vacuum for 1 h; upon meltdown and subsequent cooling down to room temperature, a purple colloid was obtained. Subsequently, upon the addition of nitrogen up to 1 atm, the colloid was allowed to warm for another 0.5 h up to room temperature. The solution was siphoned into a flask cooled in a nitrogen atmosphere from the acetone inlet. The molarity of the metal-containing solution is typically $\sim 10^{-3}$ mol dm^{-3}. During the warm-up to room temperature, clustering of metal atoms developed slowly [12, 16].

C. Incorporation of Gold Nanoparticles in VOx-NTs

6 mg of the $V_2O_5(DDA)_{0.34}$ (VOx-NTs) were refluxed with 3 ml of *n*-dodecanothiol in 15 ml of anhydrous ethanol, (fraction distillation in ethanol 98% in $CaCl_2$) for 2 h. After that, the colloidal solution with gold nanoparticles (Au-NPs) was added to acetone (average of the size of particles ∼0.9 nm). The system was then agitated for 12 h. Fig. 1 shows the synthesis schematic of the Au nanoparticle colloids. During agitation, the solvent was added in excess to ensure the solvation of the metal nanoparticles.

D. Characterization of Samples

The morphology of the vanadium pentoxide nanotubes was measured using Scanning Electron Microscopy (SEM) with a Philips XL-30 model equipped with an EDX detector and a LV-SEM JSM-5900LV equipped with a Noran Voyager EDX detector. The chemical composition of the samples were determined by elemental chemical analysis using a SISONS model EA-1108. Transmission electron micrographs was obtained on either a JEOL JEM 1200 EXII at 120 kV or a JEOL 2000FX TEM operating at 200 kV. A drop of the dispersion was placed on a 150 mesh copper grid coated with carbon. Several magnifications were used to record four to five electron images in different areas of the sample. Subsequently, 80-100 particles in each image were measured and the frequency histogram was plotted to determine the mean particle size. The Fourier transform infrared (FTIR) spectra were recorded using a KBr pellet technique on a Perkin-Elmer series 2000 apparatus in the region 4000 to 450 cm^{-1}. Raman scattering spectroscopy was conducted using a Jobin Yvon XY 800 spectrometer equipped with a cooled charge coupled device (CCD) detector. The spectral excitation was provided by an argon ion laser, using a 514.5 nm laser line (2.41 eV) with a variable laser

power density. The cathodoluminescence (CL) characterization was performed on a Gatan MonoCL 2 system operating at 10 kV.

III. RESULTS AND DISCUSSION

A. Electron Microscopy of VOx-NTs

The products of the hydrothermal treatment consist mainly of nanotubes; we observed differences in the yield with respect to report in Ref. [2] due primarily to differences in the hydrothermal treatment of the xerogel. In some rare cases, tubes of micrometer sized diameters were observed. We can attribute this observation to incomplete scrolling of the vanadate layers during the nanotube formation process [15]. The inner diameter of typical tubes varied between 20 and 100 nm and the length of the tubes was $\sim$2 μm [6, 15].

An SEM image of the synthesized VOx-NTs prior to functionalization is presented in Fig. 2. The cluster of nanotubes exhibits primarily open-ended tubes and a very uniform tubular morphology. The associated EDX spectrum shown in Fig. 2b only evidences the vanadium content of the nanotubes and the C contribution from the long-chained dodecylamine surfactant molecules. HRTEM data, shown in Fig. 3a, was acquired for nanotubes at an advanced stage of their formation. It can be observed that the sidewall regions are characterized by the 2.85 nm spacing of the lattice fringes, determined by electron diffraction measurements, as shown in Fig. 3b. This value corresponds to the d-spacing of the {100} crystal planes of VOx-NTs and is the first experimental verification of the predictions of Nesper and co-workers [2]. The central core of the nanotube is observed to be hollow and extends to the very tip. Overall, the tube is structurally uniform and from diffraction contrast in these images, the scrolling of the vanadate layers is apparent.

From TEM micrographs, the measurement of particle diameters are randomly chosen; an average of one hundred particles were counted in each micrograph to allow calculation of the average size. The histograms obtained also give useful information on the particle size distribution in the colloid. We determined that the concentration of the purple colloidal solution obtained was 4×10^{-3} mol dm^{-3}. The average particle size, as determined by TEM, is shown in Fig. 4a. By estimating the density, ρ, of Au nanoparticles as a function of diameter (shown in Fig. 4b), an average size for the Au nanoparticle diameter throughout the dispersion is estimated at $\sim$0.9 nm.

Electron diffraction measurements evidenced the polycrystalline nature of the Au nanoparticles within the tubes. The electron diffraction pattern, inset to Fig. 4a, exhibits three Debye-Scherrer rings corresponding to the {111}, {220}, and {311} planes of the fcc crystalline lattice, characteristic of randomly oriented {111} Au nanoparticles.

The stability of the colloidal suspension is $\sim$85 days, in agreement with the synthesis of metallic colloids reported previously [12, 16]. Acetone was chosen as the solvent for the Au nanoparticles as it presents a higher solvation (high stability as a function of time), compared with other metals (all obtained using the same method and solvent) such as Mn [16], Ni [13], although the colloidal particle sizes reported in this work are of smaller average diameter. Furthermore, the Au-nanoparticles/acetone metallic colloid exhibits a zeta potential, $\zeta = -6.8$ mV. Such zeta potential values indicate charge stabilization enabling an estimation of electrophoretic mobility, μ_E, for the Au-acetone colloid with a nominal concentration of 4×10^{-3} mol dm^{-3} to be $\sim 2.5 \times 10^{11}$ m^2 V^{-1}.

To allow functionalization of the interlaminar vanadate spacings with Au nanoparticles, dodecanothiol was mixed with the VOx-NTs in stoichiometric relations (thiol:amine 4:1) in a reflux reaction. Using electron diffraction to analyze the product, several vanadate inter-

laminar distances were observed. These interlaminar spacings were measured and compared with previous reports [2, 3], *e.g.* the measured distance of the {003} plane is ∼1 nm. We can also observe the presence of one center-symmetric phase (vanadium oxide) is and details are outlined in Table I.

Analysis of nanotube cross-sections was conducted using bright field TEM, shown in Fig. 5. The presence of the Au nanoparticles is not clearly visible in bright field micrograph, but by employing dark-field imaging of the Au{111} reflection (Fig. 5d), brilliant points (metallic particles) can be readily observed within the tubes. These regions correspond to areas where gold nanoparticles are present; for instance, using electron diffraction we can observe the presence of two phases in the system, one containing VOx nanotube/thiols (center-symmetric group) and the other, Au nanoparticles, shown in Fig. 5d and 5e. The corresponding electron diffraction measurements are outlined in Table II.

With this information we conclude that the gold nanoparticles are present in the vanadate interlaminar spacings. Due to the high affinity of the thiols to Au, we can surmise that the areas where the thiol molecules are present, the Au nanoparticles are also present. To determine the possibility of any preferential location for the Au nanoparticles after reflux in the acetone colloidal solution, we analyzed some areas of the nanotubes using Energy Dispersive Spectroscopy (EDX) in surface mode. Only a minute fraction of gold and sulphur is observed at the surface of the tubes, although further work is required to determine if the nanoparticles are uniquely resident in the vicinity of the thiols.

Reflux of the vanadium pentoxide product with the thiol suspension was also conducted in a non-polar medium (*n*-decane/thiol, 3/1:v/v for 2 h) containing the gold nanoparticles. The conditions of the synthesis were similar to the functionalization of the nanotubes with the thiol/acetone solution. The resulting product was analyzed by TEM and a typical

micrograph is shown in Fig. 6. TEM micrographs revealed that Au nanoparticles in a non-polar colloidal solution are not incorporated within the VOx nanotubes and only a minute quantity is sometimes observed on the outer surface, in stark contrast to observations after reflux in the acetone solution.

Analysis of dark field TEM images focusing on Au reflections revealed that the particles are trapped in the non-polar solvent at the surface and thus suggests the non-functionalization by the thiols and no subsequent incorporation of Au nanoparticles in the tubes (Fig. 6). Electron diffraction measurements revealed the presence of only one center-symmetric phase. The thiols are diluted by the non-polar *n*-decane outside the tubes; subsequently the interchange reaction with the dodecylamine is not possible because the gold particles preferentially interact with the thiols outside of the nanotubes, prior to their incorporation in the vanadate interlaminar spacings of the tubes. Thus, polar solvents are required for successful thiol functionalization of vanadium pentoxide nanotubes.

B. Raman Scattering Spectroscopy

The Raman scattering spectra the VOx-NTs containing dodecylamine are presented in Fig. 7. The single and double asterisks represent the frequencies of the breathing modes as reported in Refs [17, 18]. During acquisition, the nanotubes were targeted with laser radiation with a power density of 1312 mW mm^{-2} as slight damage was observed using laser power densities greater than 1573 mW mm^{-2}.

The xerogel exhibits a bilayered structure along the *c*-axis of the monoclinic unit cell [19]. The monoclinic unit cell typically shows a lower symmetry compared with the bulk V_2O_5 resulting in the Raman modes of the $V_2O_5{\cdot}0.6H_2O$ xerogel being observed at 291, 308, 416, 703, 881, 966, 974, and 1001 cm^{-1}. The peaks corresponding to the phonon modes of the

V=O bending vibration are observed at 291, 416 cm^{-1}.

The higher frequency modes originating from stretching vibrational modes of V−O groups (ν_{V-O}) are observed at 308 and 703 cm^{-1}. Stretching vibrational modes of the V=O group are observed at 966, 974 and 1001 cm^{-1} in agreement with the values reported in Ref. [18].

The spectra in Fig. 7 show different varieties of vibrational modes for the VOx-NTs. In the region 200−500 cm^{-1} (phonon modes), peaks located at 277 cm^{-1} and 400 cm^{-1} were observed and are related to vibrations of O atoms along the c-axis of the O−V−O bond [20].

The relatively broad mode observed with a medium strength signal at 135 cm^{-1} could correspond to the breathing mode (133 cm^{-1}) reported by Cao and co-workers [17], but this still has to be conclusively verified.

Hardcastle and Wachs [21] proposed an empirical equation to relate the highest frequency observed in the spectra with the V−O bond length in vanadium-based oxides. The relation

$$R = -\ln \frac{\omega/(21349)}{1.9176}$$

where R is the bond length in Å and ω is the frequency in cm^{-1} allows the estimation of the V−O bond length in the vanadyl group. Indeed, the nanotubes exhibit a signal at 986 cm^{-1} (medium intensity) corresponding to a bond length of 0.156 nm. This measurement is close to that measured for pentavalent V^{5+} in V_2O_5 (0.157 nm) [22]. The peaks at 683, 868 and 986 cm^{-1} show that these nanotubes exhibit an ordered structure close to that of the xerogel vanadium pentoxide [18]. Thus, these near equivalent bond length values indicate that the V^{5+} species is predominant and the comparison of the signal of the xerogel and the VOx-NTs found in the literature [17, 18] show that our nanotubes samples present an intermediate structure between a scrolled xerogel and a uniphase of VOx-NTs.

The Raman scattering spectrum of the VOx-NTs, however, exhibits a luminescence signal

in the range 1250−400 cm^{-1} with a maximum at 0.51 eV, shown in Fig. 8. This luminescence peak corresponds closely to the optical band gap of the VOx-NTs reported by Liu *et al.* [23]. Furthermore, in this spectral range (up to 1000 cm^{-1}) no observation of any first or second-order Raman modes nor combinatorial modes of vibrational overtones typically observed in other kinds of vanadium oxides [20] were detected.

The band gap of the vanadium pentoxide bulk was determined using Raman scattering at 514.5 nm and is observed to have a value of 2.1 eV. Cathodoluminescence (CL) measurements of the VOx-NTs was conducted and electron bombardment of this material does not result in any emission of light in the UV, visible, or infrared parts of the spectrum. However, the colloidal sample containing 5 nm−diameter Au nanoparticle colloids dispersed in acetone, exhibits a surface plasmon peak in the visible part of the spectrum at 535 nm and the lifetime of the excited state near the surface plasmon resonance is at most 5 ps [24], in good agreement with similar studies of other metal nanoparticles.

C. Infrared Characterization

The FTIR spectra of both the functionalized VOx-NTs and the lamellar nanocomposite are presented in Fig. 9. Signature peaks from surfactant molecules at 2917 and 2852 cm^{-1} were detected and are related to the axial stretching of aliphatic C−H groups. The band at 1462 cm^{-1} is related to the in-plane symmetric angular deformations of CH_2 species and another at 735 cm^{-1} results from the symmetric out-of-plane angular deformation of N−H species. The band at 1623 cm^{-1} is related to the N−H bending mode of the amine in the nanocomposite. The characteristic H−O−H bending mode of the water molecule was also observed [18]. In the VOx-NTs, the N−H vibrational stretching modes of the surfactant in the range 3500-3000 cm^{-1} were observed with a weak signal at 3135 and 3452 cm^{-1}. The

very weak band at 1610 cm^{-1} is attributed to the N−H bending mode of the surfactant.

Since V_2O_5 exhibits three major absorption peaks at 617, 827 and 1022 cm^{-1} [25, 26], our FTIR measurements of the lamellar organic-inorganic nanocomposite evidences the signals of the symmetric V−O−V stretch modes at 528 cm^{-1} (525 cm^{-1} for the nanotubes) mixed with the deforming vibrations of the vanadium polyhedra [23], and the $O-(V)_3$ asymmetric modes at 734 cm^{-1} [25]. At ∼1000 cm^{-1} the nanocomposite is expected to exhibit a signal from the vanadyl oxygen; our VOx-NTs present three signals in this area at 962, 1003 and 1049 cm^{-1} as the vanadate lamellar structure is composed of inequivalent V=O groups. The signal at 962 cm^{-1} suggests that the vanadium oxide is also present in minute quantities in its α-structure (V^{4+} species), the other two signals correspond to the vanadyl group, in agreement with previous reports [22, 26].

The signals of the compounds after hydrothermal treatment (HT) and the lamellar organic/inorganic nanocomposites in Fig. 9, show indeed, that the organic surfactant presents similar vibrational modes, however, it remains to be conclusively verified if the charge on the nitrogen group in the amine surfactant is altered due to the HT treatment.

Analysis of the spectra of various compounds after HT showed the presence of a medium signal in the region 3000−2800 cm^{-1} corresponding to the stretching N−H vibration of the NH^{3+} group in VOx-NTs, but the weak signal in the region 1550−1504 cm^{-1} related to the N−H bending confirms the presence of the ammonium group in the compounds after HT, confirming the observations of Nesper *et. al* [1, 4].

IV. CONCLUSIONS

We have reported a new method for VOx-NT functionalization by the interchange of long alkyl amines with alkyl thiols. This reaction was followed using gold nanoparticles

prepared by the Chemical Liquid Deposition (CLD) method. The average diameter of the gold nanoparticles is 0.9 nm with a stability of ∼85 days. The synthesized VOx-NTs were observed to have lengths of ∼2 μm and internal hollow diameters of 20−100 nm and were functionalized in a Au-acetone colloid with a nominal concentration of $\sim 4 \times 10^{-3}$ mol dm^{-3} and an electrophoretic mobility, μ_E of $\sim 2.5 \times 10^{11}$ m^2 V^{-1}.

Raman scattering spectra of the VOx-NTs exhibit a luminescence signal in the range 1250−400 cm^{-1} with a maximum at 0.51 eV, close to the reported optical band gap of the nanotubes. FTIR examination shows that the nanotubes exhibit an ordered structure close to that of the xerogel vanadium pentoxide. We conclude that most of the gold nanoparticles are located in the vicinity of the interlaminar adsorbed thiol molecules, to which they have a strong affinity, and not on the surface.

Interestingly, incorporation of gold nanoparticles within these nanotubes is not possible in non-polar solvents. TEM revealed that the gold nanoparticles in this case are located on the outer surface of the tubes, bound most likely by van der Waals interactions. Dilution of the thiols by a non-polar solvent outside of the tubes prevents the interchange reaction with the dodecylamine and ongoing work will elucidate the details of this observation.

Electron diffraction data shows evidence for the same phase of the VOx-NTs before and after the amine-thiol interchange reactions, implying that the tubes have not collapsed as the phases swap positions, and only the indexed planes and the centre symmetric groups change. Such a novel method allows for successful functionalization of these important nanotubular materials as potential candidates for nonlinear optical materials and charge storage devices.

V. ACKNOWLEDGEMENT

This work is supported by P*h*OREMOST, FONDECYT (Grants 1050344, 1030102, 7050081, 1040456), Science Foundation Ireland (SFI) under investigator Award No. 02/IN.1/I172, and the LME-LNLS in Brazil for technical support during SEM measurements.

[1] G. R. Patzke, F. Krumeich, R. Nesper, *Angew. Chem. Int. Ed.* **41**, 2446, (2002).

[2] F. Krumeich, H.-J. Muhr, M. Niederberger, F. Bieri, B. Schnyder, R. Nesper, *J. Am. Chem. Soc.* **121**, 8324, (1999).

[3] H.-J. Muhr, F. Krumeich, U. P. Schonholzer, F. Bieri, M. Niederberger, L. J. Gauckler, R. Nesper, *Adv. Mater.* **12**, 231, (2000).

[4] F. Bieri, F. Krumeich, H.-J. Muhr, R. Nesper, *Helvetica Chimica Acta* **84**, 3015, (2001).

[5] J. M. Reinoso, H.-J. Muhr, F. Krumeich, F. Bieri, R. Nesper, *Helvetica Chimica Acta* **83**, 1724, (2000).

[6] V. Lavayen, M. A. Santa Ana, J. Seekamp, C. M. Sotomayor Torres, E. Benavente, G. González, *Mol. Cryst. Cryst. Liq.* **416**, 49, (2004).

[7] B. Azambre, M. J. Hudson, *Mater. Lett.* **57**, 3005, (2003).

[8] B. Azambre, M. J. Hudson, O. Heintz, *J. Mater. Chem.* **13**, 385, (2003).

[9] M. J. Moghaddam, S. Taylor, M. Gao, S. Huang, L. Dai, M. J. McCall, *Nano Lett.* **4**, 89, (2004).

[10] K. Jiang, A. Eitan, L. S. Schadler, P. M. Ajayan, R. W. Siegel, N. Grobert, M. Mayne, M. Reyes-Reyes, H. Terrones, M. Terrones, *Nano Lett.* **3**, 275, (2003).

[11] B. Yang, S. Kamiya, Y. Shimizu, N. Koshizaki, T. Shimizu, *Chem. Mater.* **16**, 2826, (2004).

[12] G. Cárdenas, *J. Chil. Chem. Soc.* **50**, 603, (2005).

[13] G. Cárdenas, R. Segura, *Mat. Res. Bull.* **35**, 1369, (2000).

[14] G. Cárdenas, V. Vera, U. González, M. Navarro, *Mat. Res. Bull.* **32**, 97, (1997).

[15] C. O'Dwyer, D. Navas, V. Lavayen, E. Benavente, M. A. Santa Ana, G. González, S. B.

Newcomb, and C. M. Sotomayor Torres, *Chem. Mater.* **18**, (2006).

[16] G. Cárdenas, R. C. Oliva, *Mat. Res. Bull.* **35**, 2227, (2000).

[17] J. Cao, J. Choi, J. L. Musfeldt, S. Lutta, M. S. Whittingham, *Chem. Mater.* **16**, 731, (2004).

[18] A.G. Souza Filho, O. P. Pereira, E. J. G. Santos, J. Mendes Filho, O. L. Alves, *Nano Lett.* **4**, 2099 (2004).

[19] P. N. Tririkalitis, V. Petkov, M. G. Kanatzidis, *Chem. Mater.* **15**, 3337 (2003).

[20] Z. V. Popovic, M. J. Konstantinovic, R. Gajic, V. N. Popov, M. Isobe, Y. Ueda, V. V. Moshchalkov *Phys. Rev. B* **65**, 184303-1, (2002).

[21] F. D. Hardcastle, I. E. Wachs, *J. Phys. Chem.* **95**, 5031, (1991).

[22] N. Pinna, M. Willinger, K. Weiss, J. Urban, R. Schogl, *Nano Lett.* **3**, 1131, (2003).

[23] X. Liu, C. Taschenr, A. Leonhardt, M. H. Rummeli, T. Pichler, T. Gemming, B. Buchner, M. Knupfer, *Phys. Rev. B* **72**, 115407, (2005).

[24] K. Puech, W. Blau, A. Grund, C. Bubeck, G. Cárdenas, *Opt. Lett.* **20**, 1613, (1995).

[25] W. Chen, L. Q. Mai, J. F. Peng, Q. Xu, Q. Y. Zhu, *J. Mater. Sci.* **39**, 2625, (2004).

[26] M. L. Rojas-Cervantes, B. Casal, P. Aranda, M. Saviron, J. C. Galvan, E. Ruiz-Hitzky, *Colloid Polym. Sci.* **279**, 990, (2001).

Figure Captions

Fig. 1

(a) Schematic representation of the synthesis procedure for the gold colloid suspension. (b) Schematic of amine-thiol interchange reaction and functionalization of VOx-NTs with Au nanoparticles.

Fig. 2

(a) SEM image of a cluster of VOx-NTs showing the hollow center and open ends. The nanotubes exhibit uniform structure and open ended diameter dimensions. These nanotubes are typically several micrometers long. (b) EDX spectrum of the nanotubes before functionalization. The Si-K_α peak at 1.7 keV arises from the sample holder.

Fig. 3

(a) High resolution bright field TEM image of fully developed nanotubes acquired at Scherzer defocus. Lattice planes are clearly resolved at the sidewall regions. The hollow center extends to the tip of the nanotube. From diffraction contrast variations, evidence for the scrolling of the laminar V_2O_5 nanocomposite is clearly visible. (b) Associated selected area electron diffraction pattern evidencing the 2.85 nm lattice spacing at **U**.

Fig. 4

TEM image of gold nanoparticles in acetone and corresponding histogram ([Au]: 4×10^{-3} mol dm^{-3}). Gaussian and Lorentzian line fits of the are overlaid for comparison giving an average value of 0.9 nm for nanoparticle diameter. (inset) Electron diffraction pattern and

dark field TEM image for randomly dispersed gold nanoparticles.

Fig. 5

(a) Bright field TEM image of VOx-NTs after the reflux reaction with thiols (b) associated electron area electron diffraction pattern (c) higher magnification magnification TEM image (d) corresponding dark field TEM image of the NTs containing Au-NPs and thiols (e) associated electron diffraction pattern (f) inverse colour dark field micrograph showing the concentration of Au nanoparticles within the nanotubes.

Fig. 6

TEM image of the vanadium pentoxide structure with surface located gold particles. Variable focus imaging confirmed that no Au-NPs exist within the tubes. (inset) Higher magnification image showing the tip of the structure highlighted in the upper image. The arrows indicate the positions of individual gold nanoparticles on the surface.

Fig. 7

Raman Scattering spectra of VOx-NTs containing dodecylamine acquired at room temperature. The single and double asterisk represents the frequencies of breathing mode as reported in Refs [17, 18].

Fig. 8

Raman luminescence spectrum of vanadium pentoxide nanotubes containing dodecylamine acquired at room temperature.

Fig. 9

FTIR spectra of the VOx-NTs (dodecylamine) and the lamellar precursor nanocomposite acquired at room temperature between 3200 and 450 cm^{-1}.

d_{hkl}/nm	Diffraction Plane	VOx Standard* d_{hkl}/nm
1.07	{003}	0.91
0.26	{210}	0.27
0.18	{310}	0.19
0.13	{420}	0.13

TABLE I: Electron diffraction indexation of the phases of $V_2O_5(DDA)_{0.3}$ with *n*-dodecanothiol.

* In agreement with Ref. [2]

Phase	d_{hkl}/nm	Diffraction Plane	Au Standard d_{hkl}/nm
Au	0.31	{111}	0.23
Au	0.22	{200}	0.27
Au	0.12	{220}	0.14
VOx-NTs	2.51	–	–

TABLE II: Electron diffraction indexation of the phases of $V_2O_5(DDA)_{0.3}$ with *n*-dodecanothiol/gold nanoparticles.

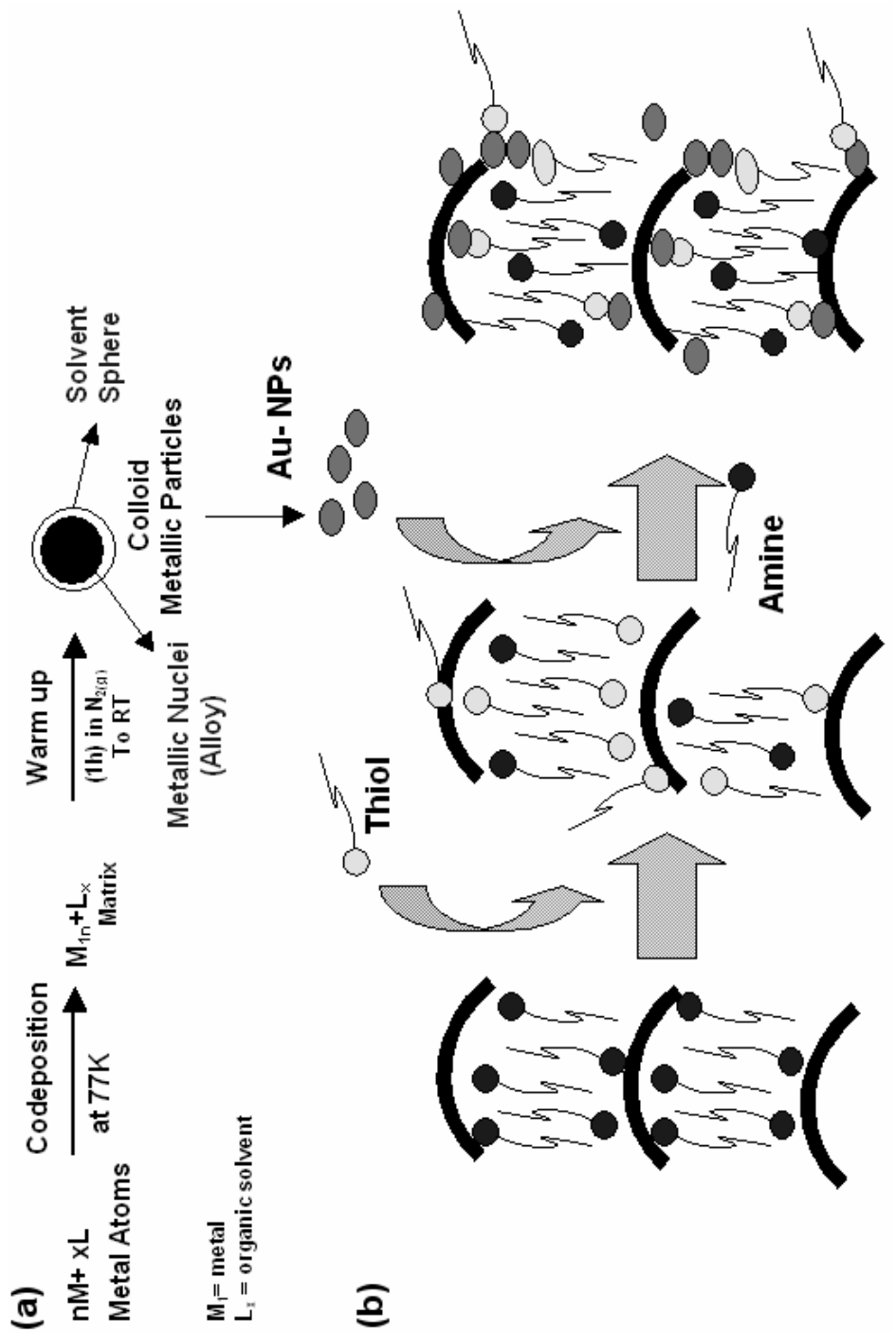
(a)
nM+ xL
Metal Atoms
Codeposition
at 77K
$M_{1n}+L_x$
Matrix
Warm up
(1h) in $N_{2(g)}$
To RT
Solvent
Sphere
Colloid
Metallic Particles
Metallic Nuclei
(Alloy)
Au- NPs
M_1= metal
L_1 = organic solvent
(b)
Thiol
Amine

Fig. 1

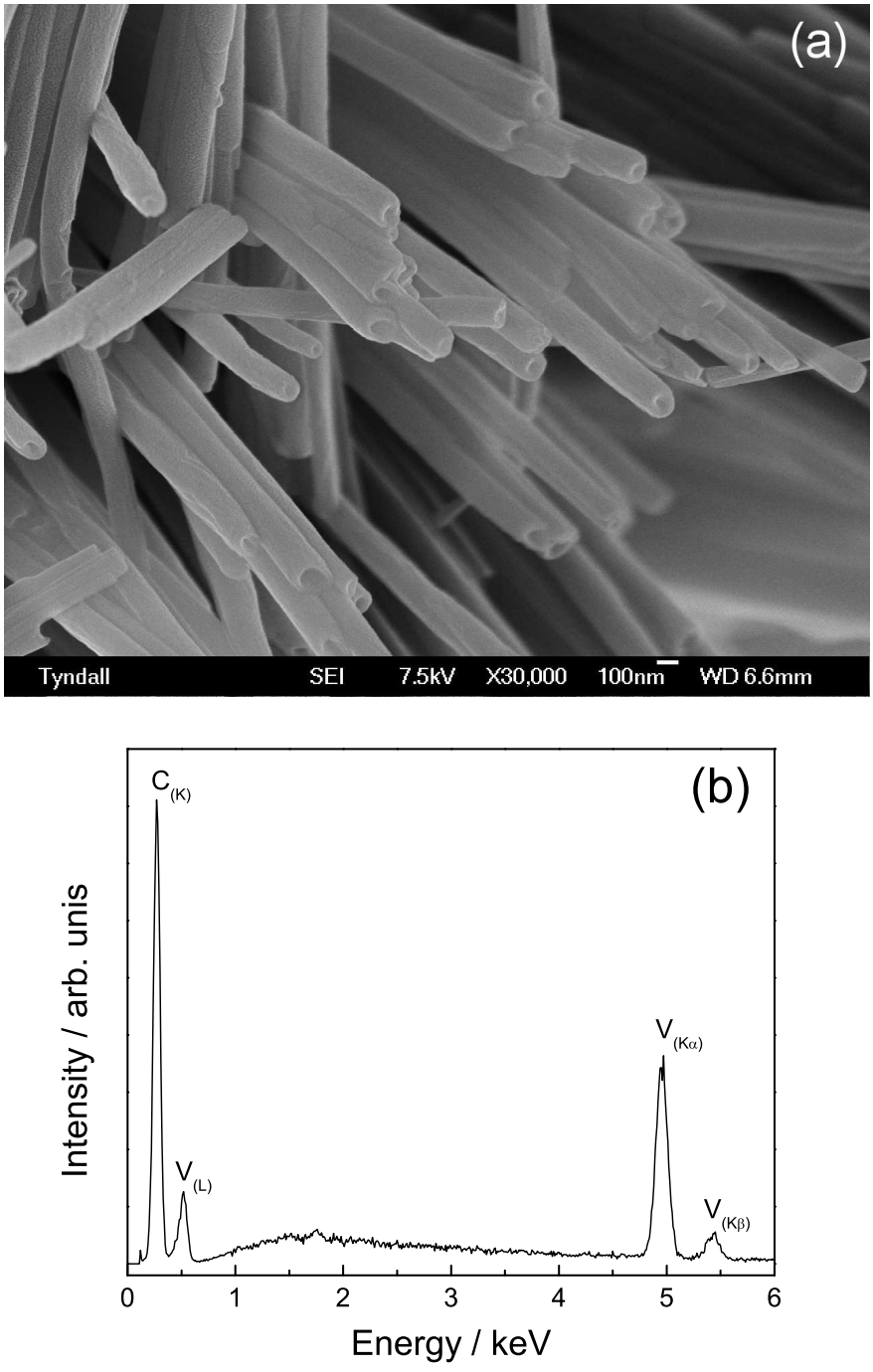
(a)
Tyndall
SEI
7.5kV
X30,000
100nm
WD 6.6mm
(b)
C(K)
V(L)
V(Kα)
V(Kβ)
Intensity / arb. unis
Energy / keV
0
1
2
3
4
5
6

Fig. 2

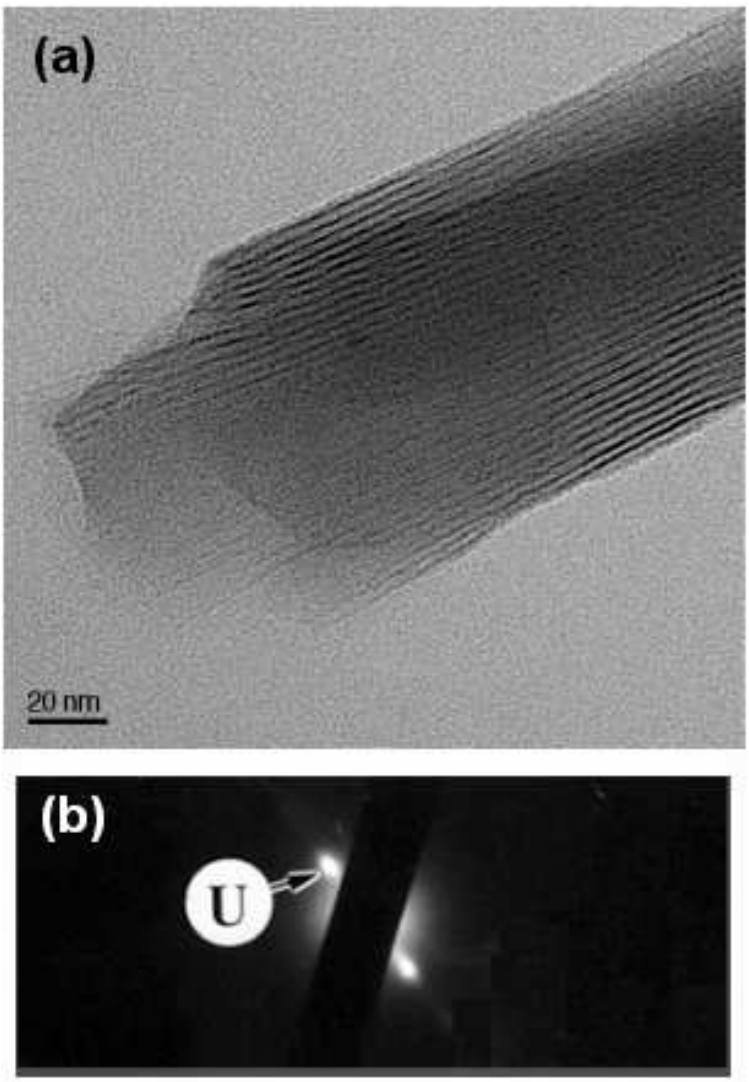

Fig. 3

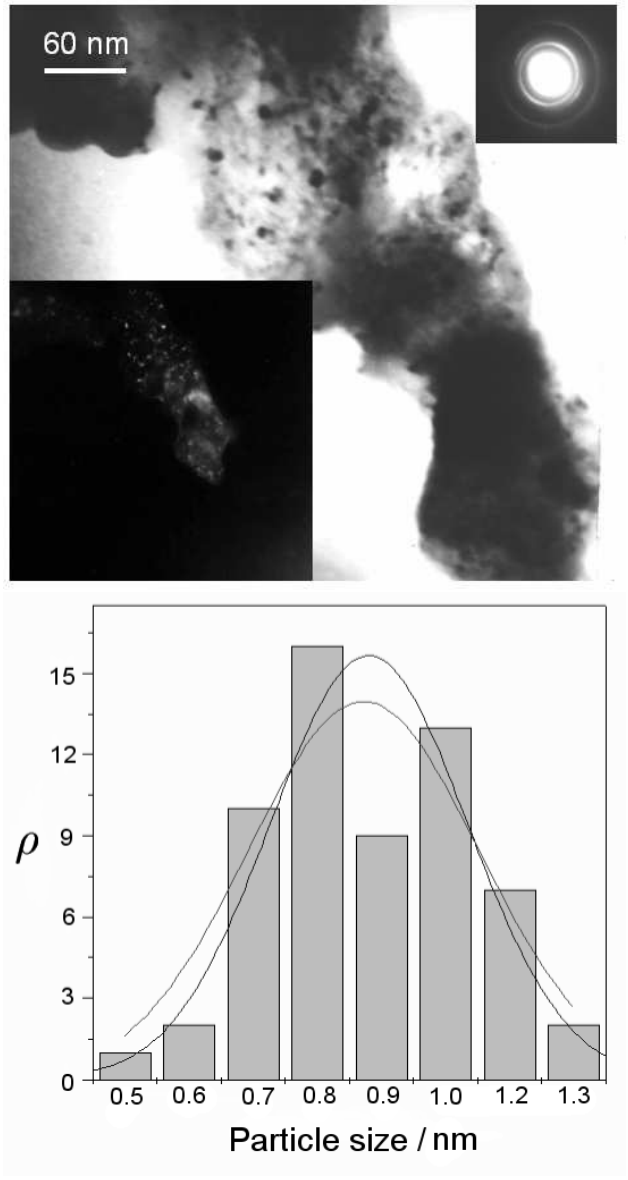

Fig. 4

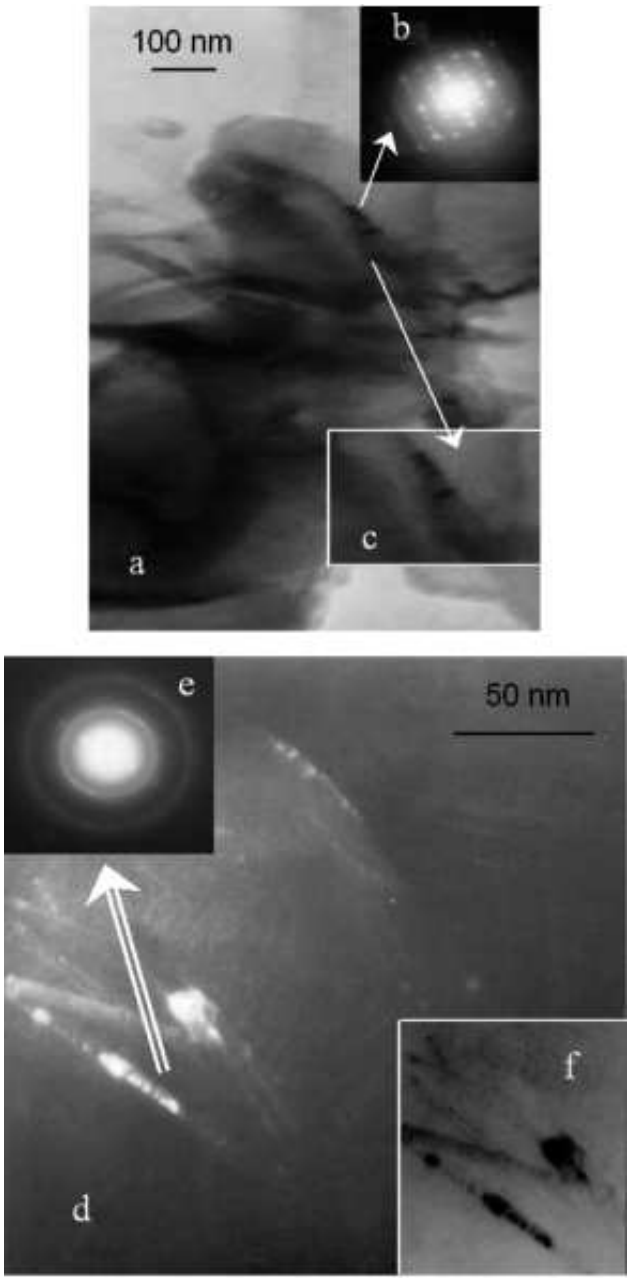

Fig. 5

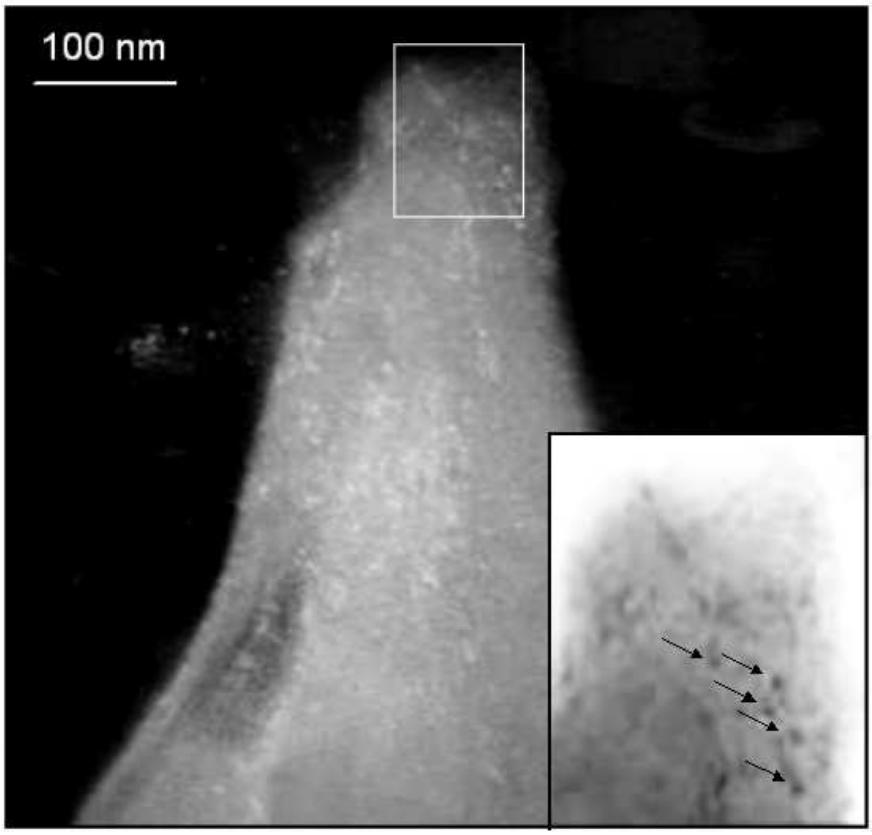

Fig. 6

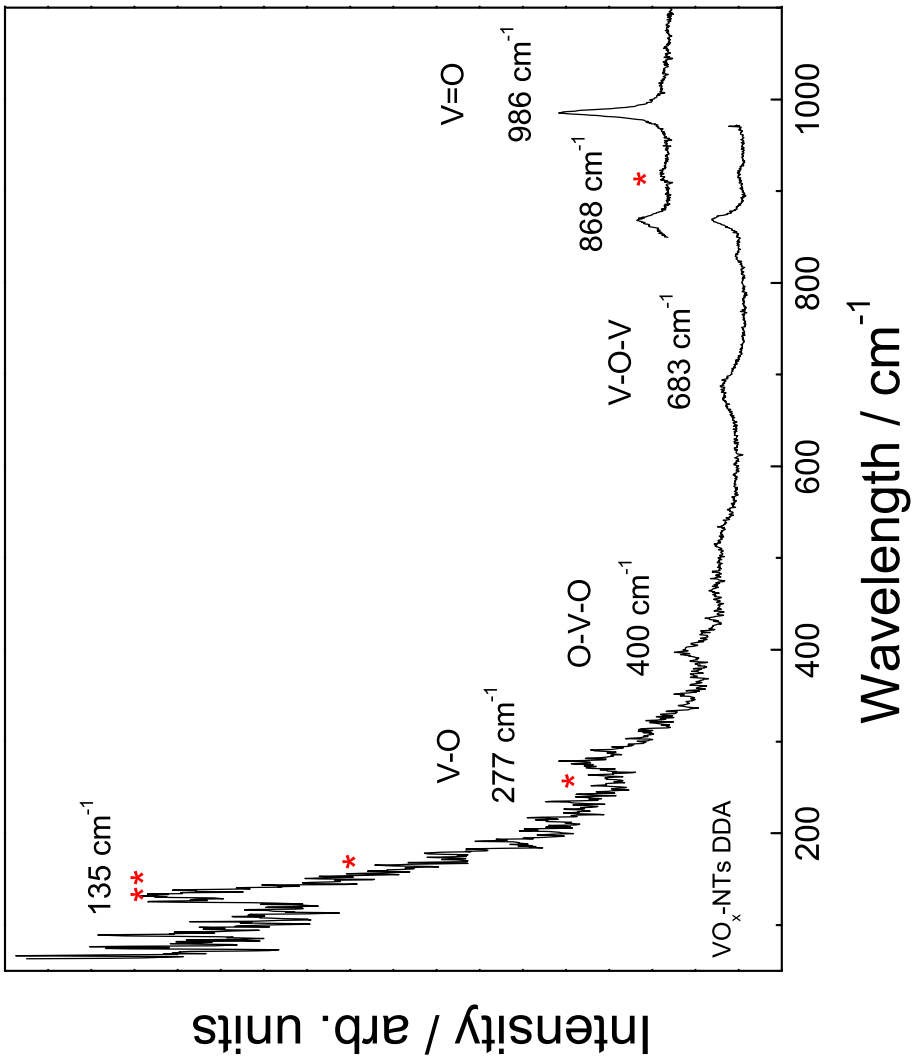
Intensity / arb. units
Wavelength / cm-1
200
400
600
800
1000
VOx-NTs DDA
135 cm-1
277 cm-1
V-O
400 cm-1
O-V-O
683 cm-1
V-O-V
868 cm-1
986 cm-1
V=O
*
*
*
*

Fig. 7

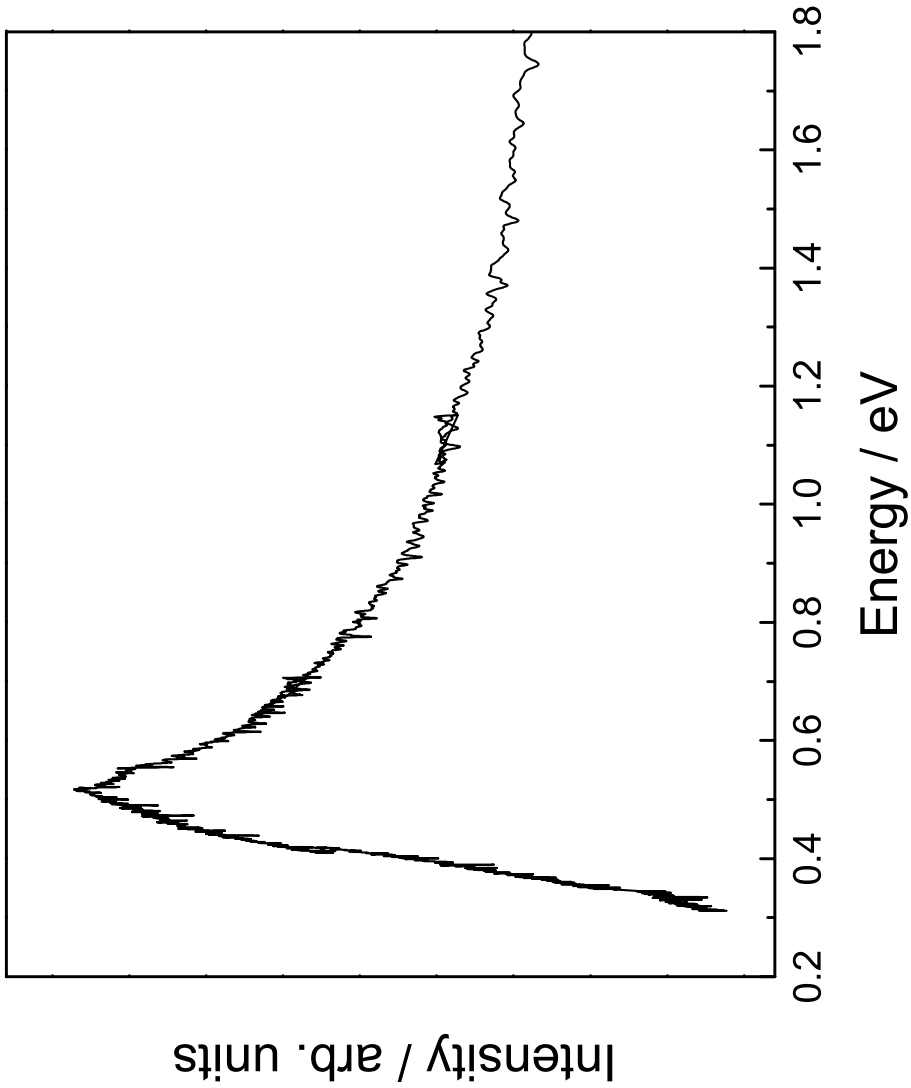

Fig. 8

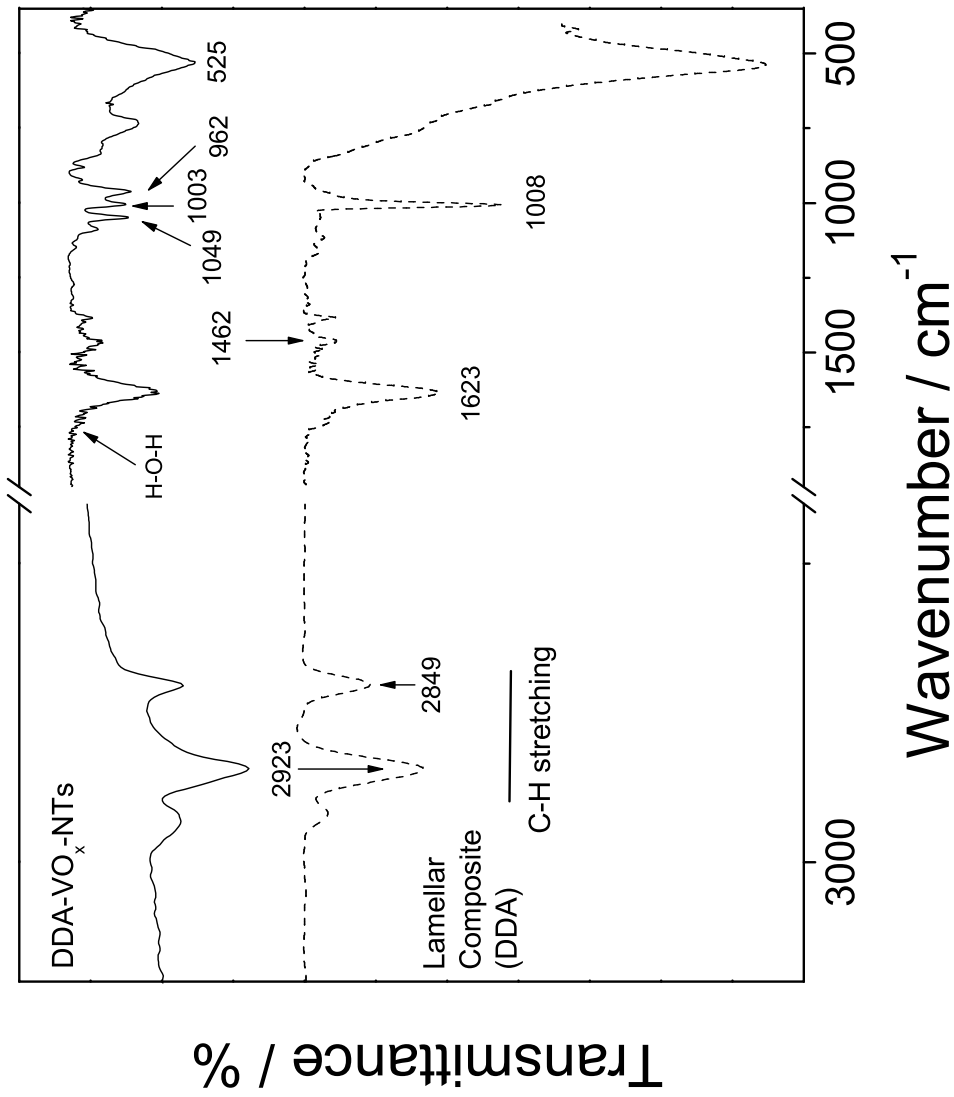
DDA-VO$_x$-NTs
H-O-H
525
962
1003
1049
1462
2923
2849
1623
1008
Lamellar Composite (DDA)
C-H stretching
3000
1500
1000
500
Wavenumber / cm^{-1}
Transmittance / %

Fig. 9